PERFORMANCE OPTIMIZATION OF INTERACTING SAILS THROUGH FLUID STRUCTURE COUPLING

V.G. Chapin[1], N. de Carlan[1, 2], P. Heppel[2]

[1]Institut Supérieur de l'Aéronautique et de l'Espace, Université de Toulouse, France
[2]Peter Heppel & Associates, Port-Louis, France

SUMMARY

In this paper, we address the problem of sailing yacht rig design through the development of a computational framework based on viscous CFD modelling for the aerodynamic part and on a non linear structural modelling for the structure part. The FSI coupling used is a loose coupling. The interest but also the expertise needed to use RANS based viscous CFD for the aerodynamic modelling is justified through examples and validations with a focus on complex separated flow configurations. The originality of the presented computational framework is its ability to address complex, non linear optimization problems with a derivative free evolutionary strategy. This capability is enhanced by the fact that it is based on a remeshing technique rather than on a deforming mesh one. After the description of the main elements of this computational framework for FSI, it is used for generic sail optimization problems and for the rig design of a 18 footer to illustrates its capabilities and limitations to produce accurate aeroelastic solutions on sailing yacht rigs.¶

NOMENCLATURE

β - Apparent wind angle
c - Sail chord
C_d, C_l - Drag and lift force coefficients
C_r - Driving force coefficient
C_h - Heeling force coefficient
C_p - Pressure coefficient
δ - Sail trim angle
δ_{GV} - Mainsail trim angle
δ_f - Foresail trim angle
f - Sail camber
F_h - Aerodynamic heeling force
F_r - Aerodynamic driving force
i - Aerodynamic angle of attack
M_c - Aerodynamic heeling moment
S - Sail surface
x_f - Location of the sail maximum camber
V_A - Apparent wind velocity

1. INTRODUCTION

The design of interacting sails for highly competitive sailing yachts is a multidisciplinary design problem addressed by sail designers, sailors and scientifics from years [1]. Sail design is an art using considerations from membrane structures and aerodynamics. The sail designer is interested to better know the global three-dimensional flow around sails with particular attention on wakes and peculiar phenomena linked to rig layout. He is interested to have a quantitative analysis of aerodynamic loads and structural stresses and their dependency to design changes. This is part of the design process.

Historically, many papers address a part of these questions from various scientific points of view [2-22]. These researches put some light on sail designer questions and their main parameters like sail aspect ratio, camber, entry angle, optimal angle of attack, sail interaction, mast effect, coupling mechanism between the mainsail and the foresail, upwind and downwind sailing conditions, sail twist and atmospheric boundary layer, flow separation, fluid structure interaction, etc...

In a more general sense, this membrane design problem is a complex multidisciplinary problem at the crossroads of the research developments needed in fluid structure coupling with numerous fields of application. This complex and multidisciplinary problem imply that various approaches are currently in development with various hypotheses. Rigorous comparisons between each of them are of high benefit to promote a critical mind in a community where passion is sometimes dominant.

For the aerodynamic part of the FSI problem, existing tools that are based on inviscid modelling and those that are based on viscous flow modelling.

Velocity Prediction Programs (VPP) that are frequently used in sailing yacht design are based on simplified aerodynamic and hydrodynamic models to predict aero-hydrodynamic forces and there dependences to design parameters. These models are crude representation of the real forces acting on sailing yachts [23, 19, 24-26]. Some of their drawbacks are known to result in some misleading predictions but increase their performance is not an easy task [23, 19, 24-26]. As said before [9], experiments are probably the best method to predict theses forces by taking into account real world effects like viscous separation, unsteadiness, etc… But it is difficult to discard scaling effects during the transposition to real yachts. It is always difficult to take into account aero-structural coupling which may be important in sail design. Another difficulty specific to experiment is the ability to access all physical variables needed to better understand flow around bodies which may be helpful to guide future design.

The best aerodynamic model we have today is viscous Computational Fluid Dynamics (CFD) through RANS simulations [8, 9, 13-16]. RANS codes have two

drawbacks when used to predict forces acting on a yacht. They may be time-consuming and they need some expertise to be accurate. But, the highest time consuming task in the process is the engineer time needed to generate meshes with a high quality standard on complex geometries. These facts drive two questions to make RANS methods useful for yacht and sail designer:

- Is it possible to automate mesh generation and integrate RANS simulations into a user-friendly environment?
- Is it possible to validate RANS predictions by comparisons with experiments representative to real flow conditions?

This problem has been addressed in previous papers [15, 16] by developing a computational framework ADONF for two-dimensional aerodynamic problems. It has been shown that it was possible to resolve optimization problem about sail design and sail interactions by simulating a large number of flow configurations through high-fidelity RANS solver. Examples illustrated have been focused on questions like: how to better design and trim interacting sails, or complex rigs. How to maximize a given function like driving force chosen to evaluate the sailing boat performance and taking into account some constraints like the maximum heeling moment?

In this paper, the extension of the computational framework ADONF is proposed to address three-dimensional FSI problem.

The fluid model is briefly presented in its main components and key elements for accurate results. The structural model is described with a special attention to the fluid structure interfacing methods used. The computational framework and the optimization algorithm are also described. Then examples are used to illustrate capabilities of ADONF for sail design and optimization with an FSI formulation for three-dimensional flows.

2. FLUID MODEL

In this section, main elements of the computational model are described. Fluid dynamics equations used to simulate the flow around interacting sails are presented with the solver and physical models and limitations. Viscous Navier-Stokes equations on hybrid meshes with structured and unstructured mesh and conformal or non-conformal interfaces between domains have been used. This is a powerful technology which increases flexibility to generate high quality meshes around interacting sails for two and three-dimensional flows.

2.1 GOVERNING EQUATIONS FOR FLUID

The viscous flow modelling around interacting sails is based on the numerical resolution of the following Reynolds Averaged Navier-Stokes equations:

$$\frac{\partial \rho}{\partial t} + \frac{\partial}{\partial t}(\rho u_i) = 0$$

$$\frac{\partial}{\partial t}(\rho u_i) + \frac{\partial}{\partial x_i}(\rho u_i u_j) = -\frac{\partial p}{\partial x_i} + \frac{\partial}{\partial x_j}[\tau_{ij} + R_{ij}]$$

With the viscous stress tensor

$$\tau_{ij} = 2\mu\,[S_{ij} - \frac{1}{3}\frac{\partial u_k}{\partial x_k}\delta_{ij}]$$

the deformation tensor

$$S_{ij} = \frac{1}{2}(\frac{\partial u_i}{\partial x_j} + \frac{\partial u_j}{\partial x_i})$$

and the turbulent Reynolds stress tensor R_{ij} which should be modelled (see turbulence modelling part). Following Boussinesq hypothesis this tensor may be approximated by:

$$R_{ij} \cong \mu_T\,[S_{ij} - \frac{2}{3}\frac{\partial u_k}{\partial x_k}\delta_{ij}] - \frac{2}{3}(\rho k)\,\delta_{ij}$$

2.2 SOLVER

The solver used for the resolution of the Navier-Stokes equations is Fluent. It is a steady or unsteady, compressible or incompressible, three-dimensional solver which resolve the previously given Reynolds Averaged Navier-Stokes (RANS) equations. In the present study, the segregated solver and the Spalart-Allmaras turbulence model [27] in its vorticity-based or strain-vorticity-based production term have been used. When not explicitly specified, second-order spatial and temporal schemes were used in its steady version and the importance of that point will be shown in result section.

To solve the Navier-Stokes equations, proper boundary conditions are required on all frontiers of the flow domain. At wall boundary, the no-slip condition is applied. A pressure outlet boundary condition is applied at the outlet. A symmetry boundary condition is used on the top and bottom faces of the domain. A velocity inlet boundary condition is applied on other frontiers (inlet, leeward and windward).

2.3 MESH ISSUES

The mesh generation is a crucial step in the process of RANS simulation. It is a time consuming activity which need engineer experience and long practice to rigorously clean the CAD geometry and do the best choice for the mesh topology and generation. The mesh influence on the results on typical sails configurations may be important and should be carefully evaluated and bounded by relevant choices in mesh size and distribution over the flow domain. Boundary layers have to be resolved on bodies (mast and sails) and this impose some criteria on mesh size in the normal and tangential direction to walls. Flow gradients should be well resolved. This may be a difficult task on typical sails

because of the zero thickness and the subsequent leading-edge pressure gradient when angle of attack is not ideal. Based on these constraints, hybrid mesh technology may be a critical issue for high-fidelity RANS simulations [13].

In fact, results are never totally independent to the chosen mesh. The relevant question when interpreting RANS results on sails is: how bounded is the mesh influence on physical quantities of interest and the required precision. This should be investigated on simplified geometry through validation with wind-tunnel results [13].

To illustrate the mesh convergence, figure 1, the lift-to-drag ratio convergence with mesh number of points on a typical sail (f/c = 12.5%, Re = 1.4 x 10^6) calculated on four meshes have been shown. On this particular example, a good convergence on a critical physical quantity may be observed.

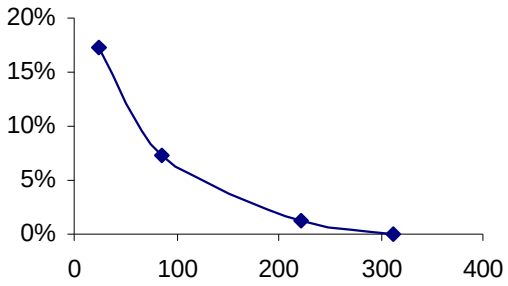

Figure 1: lift-to-drag ratio convergence with mesh refinement (number of points divided by 1000

Another important feature of mesh is their flexibility to be used with different kind of sail geometries and trim angles. A critical point for yacht rig aerodynamic studies is the necessity to generate meshes on multiple bodies (mast, mainsail, jib, etc…) which interact and may be displaced relative to each others. The challenge is to generate good quality meshes in the boundary layers regions of each body without using too high aspect ratio cells which may generate numerical scheme instability and too much grid points for computational efficiency reasons. To respect these topologic constraints and obtain good mesh control, hybrid meshes (figure 2) is a useful technology. For more flexibility, it may be completed by non conformal interface between the inner structured region around masts and sails and the outer unstructured region around all interacting structured domains (figure 2) as was done with Gambit 2 [28]. The mast trailing-edge with link to the zero-thickness sail is a region of difficulty for the structured mesh part and need much more attention and some tricks.

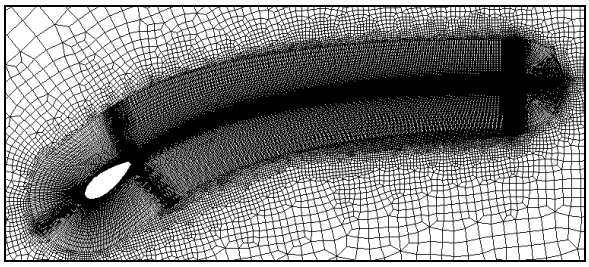

Figure 2: hybrid mesh example

2.4 TURBULENCE MODELING

Sail aerodynamic is highly concerned with separation bubble, turbulent transition and turbulent reattachment process and it is well known that these phenomenon and their associated pressure losses may have a critical influence on pressure and friction distribution on sails. Also an accurate representation of laminar and turbulent separated flow regions is critical when we are concerned with drag prediction.

In a previous paper [14] detail flow analysis with separation regions on mast and mainsail configurations have been computed and for validation purposes. Comparisons were made with wind-tunnel results of Wilkinson [29-31]. It has been shown that the Spalart-Allmaras turbulence model may have coherent qualitative behaviour on mast-sail geometries and may reveal to be better than more sophisticated turbulence models based on two transport equations.

The Spalart-Allmaras turbulence model used in this paper is a one equation model with standard coefficients values. The equation is a transport equation for the turbulent viscosity as follow:

3. STRUCTURE MODEL

The structural modelling is based on the software RELAX. It is an interactive, fully non-linear finite-element code to analyse fabric structures using a state of the art relaxation method. RELAX special sail analysis features enables it to predict the behaviour of almost any large-displacement structures. It is a good candidate for sail analysis through a fluid-structure loop.

The method of resolution is based on Barnes studies [32], using dynamic relaxation and kinematics damping. The model is based on membrane elements for sail modelling and beams elements for battens. This model is described like a parametric surface (u,v local coordinates). Sails materials can be described as a composite material: each ply contains a filament laid or a film. The behaviour of the material can be non linear. Resolution method is based on an explicit scheme with a first order time and space discretization.

RELAX has a sophisticated meshing tool which can automatically mesh sail geometry given by a CAO software, such as RHINO 3D. Sail meshing is realized using Delaunay triangulation. The grid relates to boundaries of panels and is refined in regions of greatest

curvature. During analysis nodes move to their new equilibrium position. There is no remeshing of the structure.

Knowing that a membrane element has no resistance in compression, a wrinkling model is implemented in RELAX to take into account the compressive stresses. As a membrane has an infinite number of kinematics degree of freedom (possibility to deform without a change of stress) and a grid has a finite number of kinematics degrees, the wrinkling modelling allows a better prediction by adding freedom degrees. At that time, the membrane is considered as an orthotropic material with a linear behaviour.

RELAX is a robust solver but excess material which is not supported by a batten is a source of instability. This is a consequence of the choice of membrane elements which have no resistance in bending. Also, extended foot modelling can be problematic.

RELAX interface presents various possibilities of trimming. This is useful to modify sail shape in a realistic way. In particular, halyard, stay and clew length can be changed, as carriage location.

All data are saved from the last analysis. This is a useful point in the case of FSI loop. From a loop to the next one, just the pressure field has to be updated while stresses, geometry and mesh are conserved in memory by the soft. This allows saving computing time.

4. FLUID STRUCTURE COUPLING

With actual computing power and accessibility of specialized software, it is now possible to predict flying shape of sails through FSI coupling [18]. The resolution in the same time of aerodynamic and structural equations is the best way to join this goal but it is a computationally expensive way [41]. A loose coupling method allows a reasonable prediction with smallest means by using specialized software for the fluid and the structural part.

4.1 PRINCIPLE

In a loose coupling method, aerodynamic and structural equations are solved independently. It is possible to use two different software, one dedicated to structural analysis and the other dedicated to fluid analysis even if they are not developed to communicate together. Once the loop initialized the structural code send to the fluid code the data concerning the sail shape and the fluid code send it back the pressure field on sail surfaces. Iterations are made until convergence.

4.2 INTERFACING

The aerodynamic and structural solvers are different and don't have the same needs concerning the meshing. So there respective meshes are totally independent and an efficient interfacing method needs to be developed to link these modules. In the FSI loop, the aerodynamic solver sends the pressure field on the geometry to the structural solver and the structural solver communicates the new shape of the geometry resulting from the given pressure field. Also it is necessary to provide a mapping of the pressure field from the fluid mesh to the structural mesh with no prior knowledge of the target mesh.

To achieve this, the coordinate of the structural surface is mapped onto the unit square using a development of the texture-mapping method described in Desbrun [33].

When the structural mesh geometry is exported for CFD, we also save a record of the relation between the texture-map coordinates and the current global Cartesian coordinates. We do this by constructing a NURBS surface approximating the structural model with surface parameterization chosen to match the texture coordinates. This provides a good record of the relation between global Cartesian and texture coordinates, although the tensor product NURBS surface cannot capture all the shape details. This NURBS surface is saved in a neutral CAD format.

The CFD typically returns a surface pressure field at global Cartesian positions of the fluid mesh. For each pressure sample point, we associate the pressure value to texture coordinates by finding the closest point on the NURBS surface. This operation is loss-less because every pressure sample is mapped. It introduces position errors of order of the square of the error the NURBS approximation.

Then the new sail shape corresponding to this pressure field is given by the structural solver using an iges file. The new sail shape is used by the aerodynamic mesher to generate a new mesh instead of using a grid moving technique. This choice is more time consuming than moving grid techniques but it is more robust for large displacement membranes and small cells necessary on sail boundary layers for accurate pressure field prediction. The meshing time is about 10% of the calculation time, which seems reasonable.

4.2 LIMITS

This type of loose coupling FSI is not a perfect solution [41]. Maintaining accuracy in data exchanges between structural and aerodynamic software is important to obtain relevant aeroelastic results but it is not easy. Stability can also be a problem in particular when aerodynamic stiffness and structural stiffness are of the same order. Tests and comparisons are necessary to evaluate different coupling techniques.

5. COMPUTATIONAL FRAMEWORK

Fluid motion around deforming and interacting sails in their real environment is a complex non linear problem. This may be more complex if separated flow sail configurations with unsteady phenomena related to

deformations and wrinkling are considered. Because there are a lot of parameters that define a complete rig design, there is a crucial need to integrate and automate the entire simulation process. If this is done, it will be easier to understand flow physics and gain insight for better rig design and trim. Turnaround time of the simulation process is a major constraint in common use software. *ADONF* is a response to this problem. It gives us the ability to analyse or optimize a large number of rigs configurations. It opens a new way to the design process by using a computational framework. It proposes to enhance the classical design process, which is rather based on the designer experience and a trial and error process, by a computational design process able to explore the design space through the resolution of an optimization problem.

ADONF is a computational framework which integrate and automate the entire computational environment for flow simulation from CAD definition, to mesh generation, flow simulation, flow analysis and design modifications using an optimization loop. This optimization loop is symbolically described on the diagram of figure 3. The main bottleneck is the mesh generation process automation. But it is also a critical advantage over hand made mesh generation as it generates meshes of high reliability and reproducibility. This specific property of automated meshes increases our ability to compare and rank different design or sail trim. It also increases ease to study the mesh density influence on results.

As it will be shown through examples, in the next section, it becomes possible to investigate and resolve new questions about fluid motion around designed bodies and their related performances.

The first level of new questions that can be investigated is the "what-if" questions. What will be the performance of this rig design if I change the mast section? What will be the performance of this rig if I change the sail overlapping factor preserving a constant sail surface? Etc… Only sail designer imagination and time limits the process.

For the second level of questions, optimization algorithms have been implemented in *ADONF*. With optimization algorithms, a second set of questions becomes open for sail researches or sail design. How to change the rig design or the deck plan to increase the performance of that particular sailing boat in given wind conditions? How to change rig trimming to increase boat speed in given wind conditions? What is the best camber and trim of these two interacting sails to maximize driving force or driving to heeling force ratio? Etc… This will be illustrated in more details through examples in the results sections.

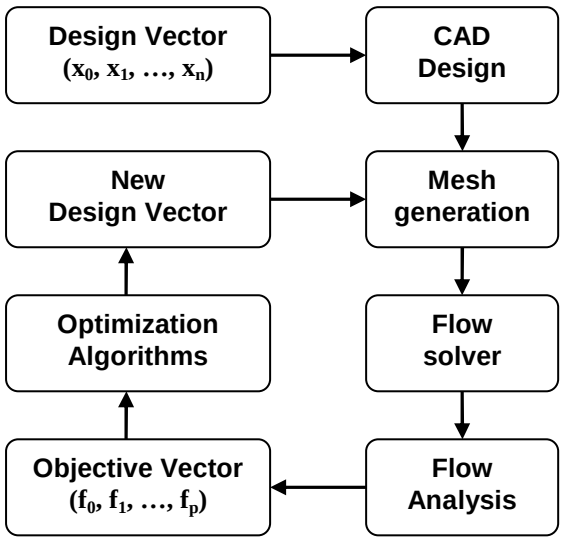

Figure 3: *ADONF* optimization diagram

6. OPTIMIZATION ALGORITHM

Many optimization algorithms may be used depending on the properties of the objective function in the explored design space. Gradient or simplex methods are well known optimization algorithms. They have been used but they have some disadvantages. They may be slow to converge close to the optimum and this may be a problem when the evaluation cost of the objective function is high. This is precisely the case for CFD applications. Another disadvantage is the zigzag down valley problem but the more important problem is their dependence to initial conditions for multi-modal optimization problems. It is not easy to show if a given CFD problem may have a multi-modal objective function when the objective function evaluation is high and that the design variable number is large [35]. But in a simple optimization problem in CFD with a subset of the total design variables it has been shown that the objective function may be multi-modal [15]. It is one of the reasons we have chosen to use evolutionary strategy rather than more conventional ones.

An evolution strategy (ES) is an optimization method based on Darwinian ideas of the natural evolution. These techniques created in the early 1960s have been developed further for fluid flow problems in the 1970s and later [34].

In this paper, we use the CMA-ES (**C**ovariance **M**atrix **A**daptation **E**volution **S**trategy) evolutionary algorithm. It is well adapted for non linear non convex optimization problems in continuous domain. It is also well adapted for noisy problems when derivative based methods fail. Because it doesn't presume or require the existence of a derivative of the objective function, it is feasible on non-smooth and even non-continuous problems, as well as on multi-modal problems. Following Hansen [36] it is a particularly reliable and highly competitive evolutionary algorithm for local

optimization and also for global optimization problems [37, 38].

One more advantage of this ES algorithm is that it doesn't require a tedious parameter tuning for its application as opposed to commonly used genetic algorithms.

Now we have defined all the ingredients of our computational framework, examples will be given to illustrate the possibility it open for sailing yacht rig optimization through an aerodynamic or an aeroelastic modelling of the problem.

7. RESULTS

Results will be presented through five sections. The first section illustrates the importance of viscous flow modelling through RANS. The second, third and fourth sections illustrate the interest of optimization studies for sails. The fifth section illustrates FSI applications.

7.1 VISCOUS FLOW PREDICTION

A first point is to understand why and when viscous flow modelling is needed rather than inviscid potential flow modelling for sail design and trim.

To illustrate this point, it may be considered that only 3D sails should be of interest. In this case, one may consider Jones & al. [7]. In this study, it is shown on a IACC rig with mainsail and jibe that viscous and inviscid solutions predict opposite ranking for two sail camber design in same wind conditions. It will be of interest to know which modelling is wrong but no experimental results are given.

If one accept to consider a more simple case with only one 2D sail, it is interesting to look for the prediction of sail performances with viscous modelling for various sail camber. On figure 4 and 5 maximum lift coefficient and lift-to-drag ratio are presented versus sail camber value. It is interesting to see that viscous prediction is able to predict that there is a maximum lift value which can't be surpassed by increasing the sail camber. Viscous flow modelling predicts a limiting camber value as wind-tunnel do but as is not predicted by potential flow modelling. Another interesting result of these viscous flow simulations is that depending on the numerical scheme used it may be possible to predict a maximum lift-to-drag ratio for a sail camber around 10%. Second-order scheme predict this known result but first order one scheme doesn't.

It may be useful to know these results when more complex 3D rig configurations are analysed.

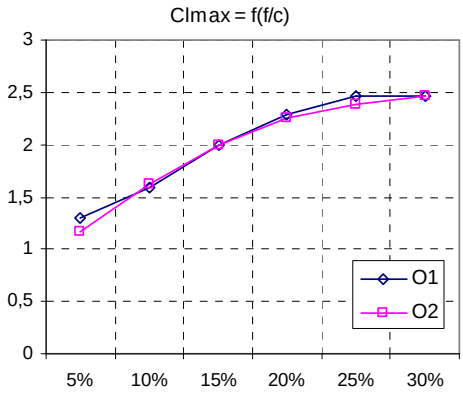

Figure 4: RANS prediction of maximum lift coefficient of a gennaker series of camber ratio ranging from 5% to 30%.

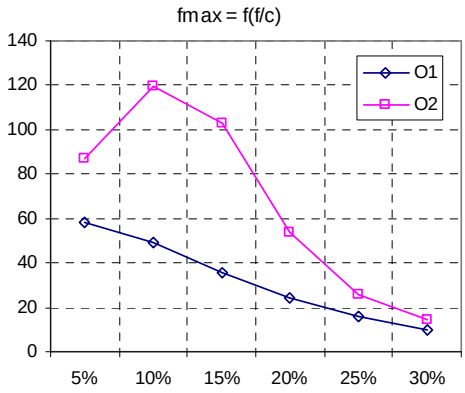

Figure 5: RANS prediction of maximum lift-to-drag ratio of a gennaker series of camber ratio ranging from 5% to 30%.

7.2 OPTIMAL SINGLE SAIL

From F. Bethwaite [40], it is known that there exists an optimum sail camber for a given mast. This observed fact has been chosen as a test case to validate *ADONF* and the implemented optimization algorithms for sail design questions.

For a single sail the optimization problem may be formulated as follow: for a given apparent wind angle, what is the optimal camber and related trim angle which maximize the driving force Fr? The apparent wind angle chosen was $\beta = 30°$. Other sail parameters are listed in the following table:

β	x_f	C	f_0	δ_0
30°	30%	6500	7%	13°

In this example, a gradient based algorithm, known as the Simplex method, is used. The optimization problem has been resolved by computing solutions based on the viscous RANS model. Twenty designs computation were sufficient to obtain a good convergence to a sail design and trim (figure 6, 7). The

following optimal solutions for maximum driving force and maximum lift-to-drag ratio has been found:

Objective	f_{GV}	i_{GV}
Max(Fr)	18%	7°
Max(Fr/Fh)	8%	3°

The number of needed RANS simulations to determine the optimal solution is dependent to the variable number. In this example with only 2 variables, the convergence to the optimal solution is fast. It has been verified, by changing the initial condition that the optimal solution was independent to the initial condition. An example of algorithm convergence is given on figures 2 & 3 for camber, trim angle and driving force.

It is interesting to note that the optimal solution, maximizing the driving force, present a separation near the trailing-edge on the suction surface (figure 8). This point clearly illustrates the ability of viscous CFD to make a trade-off, between high camber and massive flow separation on the suction side of the sail, through RANS simulations.

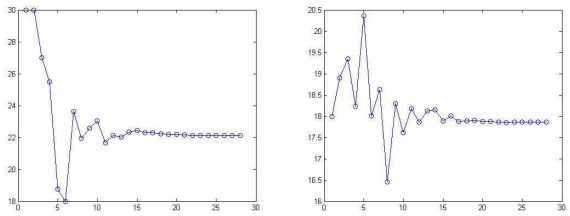

Figure 6: trim and camber convergence

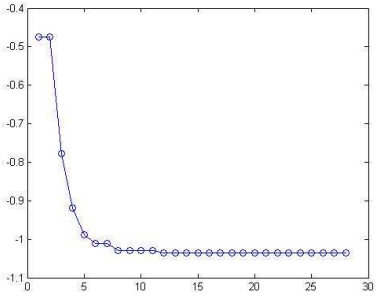

Figure 7: driving force convergence

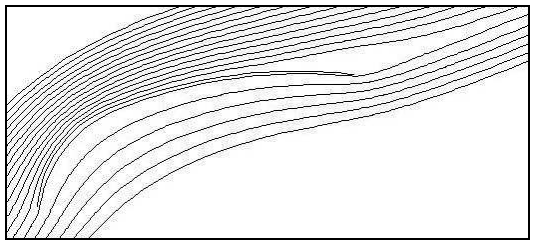

Figure 8: stream function around the sail for maximum driving force at $\beta = 30°$

7.3 OPTIMAL INTERACTING SAILS

A more challenging optimization problem is the interacting sails problem. The mainsail-jib interaction on a sailing boat is a well known problem which has generated long debates and controversies [1, 4]. The question was to know if *ADONF* may be used to explore this problem in more detail, to clarify the relation between foresail and mainsail shapes and rig performances by taking into accounts separated flows through viscous RANS modelling.

The optimization problem may be formulated as follow: for a given apparent wind angle, what are the optimal cambers and related trim angles which maximize the driving force Fr? The apparent wind angle chosen was $\beta = 30°$.

As in the previous case, the Simplex algorithm has been used. The results for the optimum design & trim are listed in the following table:

Objective	f_{GV}	f_{JIB}	i_{GV}	i_{JIB}
Max(Fr)	27%	30%	27°	-2°
Max(Fr/Fh)	4%	19%	20°	-1°

The solution that maximizes the driving force is visualized on figure 9. As in the previous case, small separation regions are found near the trailing-edge on the suction surfaces.

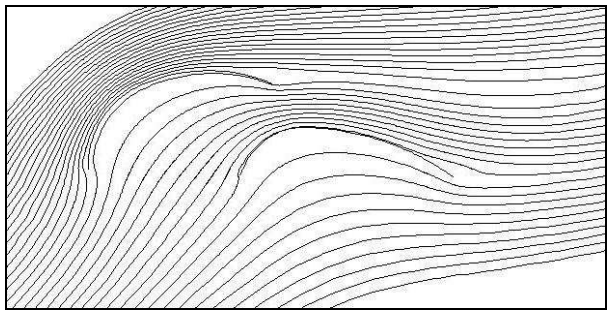

Figure 9: stream function around two interacting sails for maximum driving force at $\beta = 30°$

For further investigation, it will be possible to take into account a constraint on the heeling moment to obtain more realistic designs for a given boat. This constraint may be added through a penalty method or another constraint handling method [38, 39].

7.4 3D SAIL DESIGN OPTIMIZATION

Our computational framework ADONF has been recently extended to three-dimensional optimization. A first example of an aerodynamic three-dimensional optimization of a sail shape and trim based on viscous RANS simulations we have considered a generic mainsail in upwind conditions.

The sail optimization problem is defined as follow: search to maximize the driving force of the sail through a parameterization of her camber and trim angle on the three main sections (bottom, middle and top sections). The six variables considered for optimization

are the camber and trim angle of the three sections. In this first example no FSI loop is implemented yet. The optimization process resolves three-dimensional Navier-Stokes equations in RANS formulation with Spalart-Allmaras turbulence model and the CMA-ES evolutionary algorithm search for optimal camber and trim angle in the three sections of the sail.

The mesh is automatically generated on GAMBIT with sail surface boundary layer resolution of y+=O(300) and a total of 125 000 cells. This is a coarse but sufficient mesh resolution to test the optimization as was shown during previous tests. The resolution constraint may be relaxed during optimization because, as said before, automatic mesh generation has a high repeatability. Another reason is that we just need to rank various sail shapes not to predict there absolute performance. In fact, as shown in a previous paper, the important point is to be sure that main flow features of the explored rig configurations are well predicted [13]. At the end of the process, when the best shape is found, it is always possible to increase the mesh resolution during another RANS simulation for higher absolute accuracy.

During the optimization process, which in this small case has been stopped at 91 RANS simulations, all the sail designs tested are represented in the design space and in the performance space. The history of the optimization process may be followed. As an example, on the figure 10, the aerodynamic performance of all the tested configurations is represented in the (lift, lift-to-drag ratio) plane. Because the optimization search for maximum lift, an accumulation of tested design is clearly visible in the maximum lift region during the end of the optimization. When you see that and you think it is enough, it is time to stop the optimization process.

A subset of designs, the non-dominated designs, separates the aerodynamic performance plane in two regions (figure 10). On the left of the red curve, we see the region of accessible designs and on the right, the region of inaccessible designs (for the given optimization problem). The non-dominated solutions along the red line gives the best compromises achievable in the plane (lift, lift-to-drag ratio) with the parameterized sail studied during this optimization problem.

The friction lines on the leeward side of the sail for selected designs extracted during the optimization are shown on figure 11. On the three first sail designs, separation zones are clearly identified at the top of the sail for design 1 and 3 and in the mid-section on the design 2. On the following two sail designs (4, 5) the flow is more attached along nearly all the sail surface with only a very small separation at the top of the sail. Design 4 and 5 are not far from the optimal design 6 which show no separated zones.

This sail shape maximizes the driving force in the range tested for camber and trim angle (4%<f/c<40%, 5°<δ<25°). It is interesting to notes that for three-dimensional sails, as opposed to two-dimensional sails, the solution found by the ES optimization, which maximize driving force, is not far from a separated flow but is not separated.

Given optimization examples in two and now in three-dimensional flows illustrates what can be done on sail design with the computational framework ADONF. It may be used to quantify the influence of mainsail-jib overlapping factor, sail camber position, entry and exit angles, etc, in a simple manner.

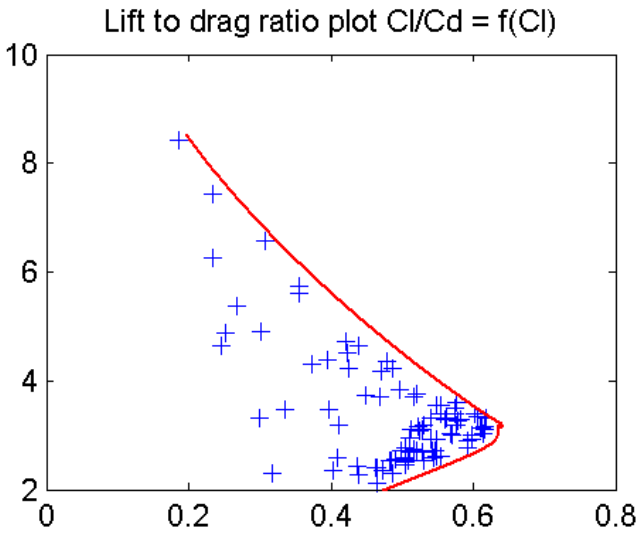

Figure 10: aerodynamic performances of all the tested sail designs during the optimization process.

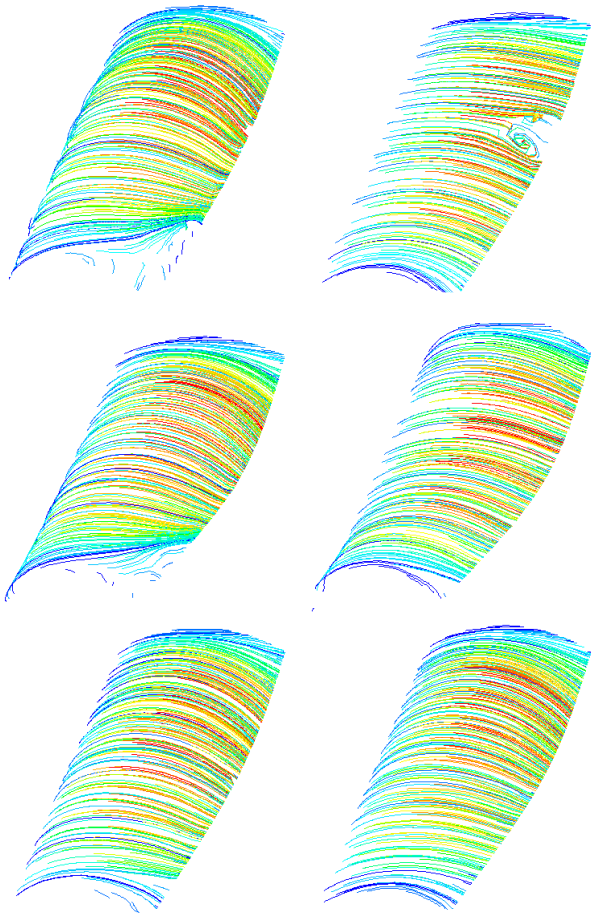

Figure 11: selected sail designs showing the convergence toward an optimal sail design.

7.5 PRELIMINARY FSI RESULTS

7.5.1 FSI ANALYSIS

As a first FSI analysis, we are considering the flow around a genoa alone in upwind conditions. This genoa design is taken first to quantify the influence of the aerodynamic model on the resultant flying sail shape and the influence of the structural model on the aerodynamic loads for two apparent wind angle (30°, 33°).

Figure 12 gives a comparison of three sail shapes. The design shape in cyan, the flying shape given by RELAX with a constant pressure aerodynamic model resulting in the same aerodynamic force and the flying shape given by RELAX with a pressure field obtained by a three-dimensional RANS calculation. Regions of differences may be observed. The stay and leech regions are important regions of differences with a high dependence of the sail entry angle to the tension of the stay. This will be seen in more details in the next section.

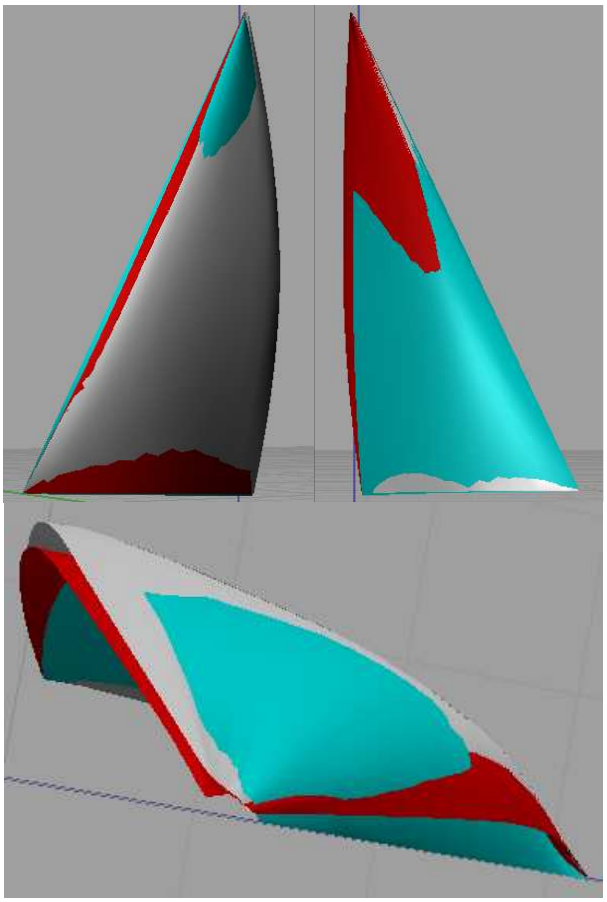

Figure 12: design shape (cyan), flying shape / RANS (grey), flying shape / p=Cte (red), (left) leeward side (right) windward side (bottom) top view

Following figures 13, 14a give a comparison of the friction lines along leeward genoa surface for two apparent wind angles (30°, 33°) on the design shape and on RANS flying shape.

Figure 13, it is seen that the flow doesn't separates on the leeward side of the sail for the lower apparent wind angle but it may be observed that separation is not far. Always on figure 13, at the higher apparent wind angle, separation take place on the lower part of the sail. For RANS converged flying shapes, it is seen on figure 14a, that the flow separates for both apparent wind angles. Separation is present only in the middle part for the lower apparent wind angle. Extension of the separation region is far larger for the higher apparent wind angle. This last case is nearly totally separated on the leeward side of the genoa.

The separation extension on the sail surface has an impact on driving and heeling forces. On design shapes, the driving force increase by 10% when apparent wind angle increase by 3° despite the separation which take place on 20% of the sail surface. On flying shapes, the driving force decrease by 20% when the apparent wind angle increase by 3° because of the total three-dimensional separation on the leeward side of the genoa.

These four visualizations of the leeward side of the genoa clearly illustrate the relative importance of aerodynamic and structural effects that may take place on sails.

Figure 14b shows friction lines on the windward side of the genoa for both apparent wind angles on the flying shapes calculated by RANS-FSI. This sail side is simpler to analyse with no strong non linear phenomena except on the bottom part of the genoa with the tip vortex (figure 15) and the top part with a high vertical velocity component along the stay which is more pronounced on the head part of the sail. This vertical component is very high for the highest apparent wind angle with a totally separated flow on the leeward side (figure 14b).

It will be interesting to observe these flow fields on the genoa in the interaction with a mainsail to have a finest understanding of the interaction consequences on the three-dimensional flow fields.

All these figures clearly show the interest of three-dimensional FSI simulations. With these detailed flow fields, it becomes possible to increase our global understanding of three-dimensional viscous flows, to observe the emergence of separated regions with design parameters variations and to quantify there consequences on aerodynamic forces and sail performances.

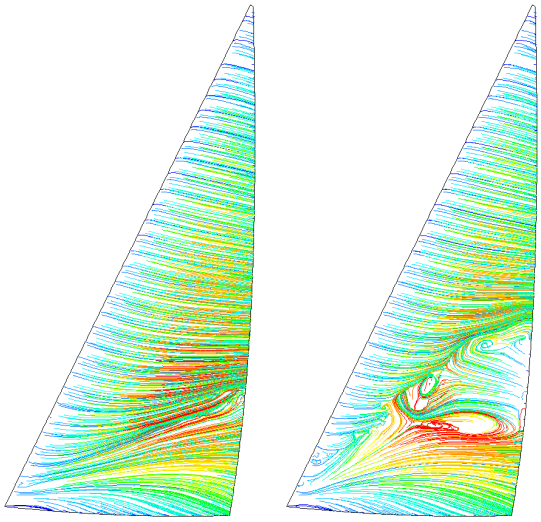

Figure 13: leeward design shape: β = 30°, 33°

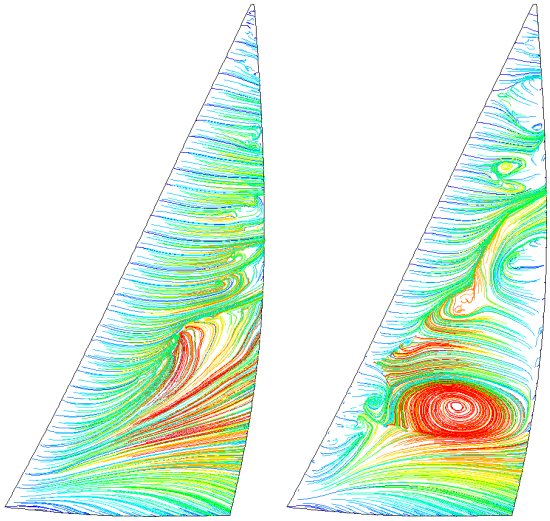

Figure 14a: leeward flying shape: β = 30°, 33°

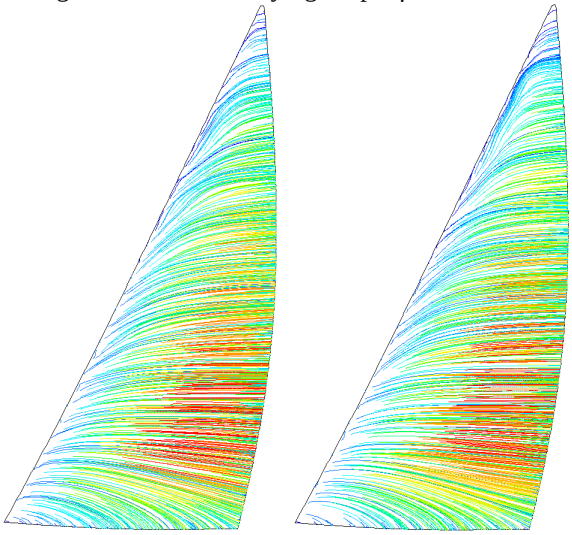

Figure 14b: windward flying shape: β = 30°, 33°

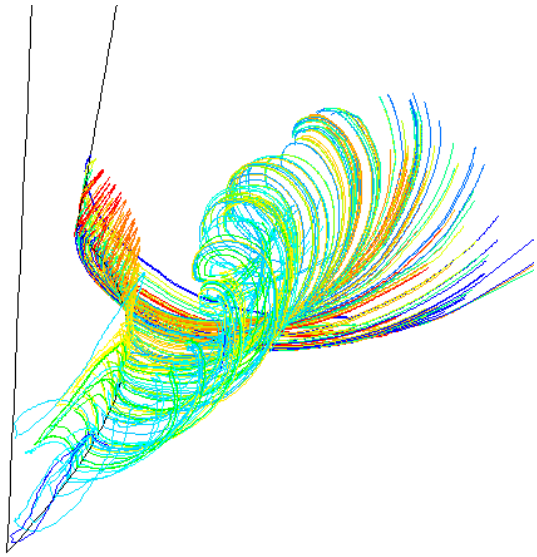

Figure 15: tip vortex on the bottom of the genoa β = 30°

7.5.2 18 FOOTER RIG DESIGN

As a second step in FSI investigation, the influences of main parameters have been quantified on the design of an 18 footer genoa in upwind sailing conditions (apparent wind V_A=20 knots, β=21°). A mainsail and a genoa are modelled but the fluid-structure interaction was studied only for the genoa. The mainsail was considered as a rigid sail (figure 16).

The genoa is first designed with all its geometric characteristics: seams, stripes, filaments, battens, reinforcements. Rhino 3D has been used to create this first model (figure 17). Mechanical characteristics are applied on each part of the sail using RELAX.

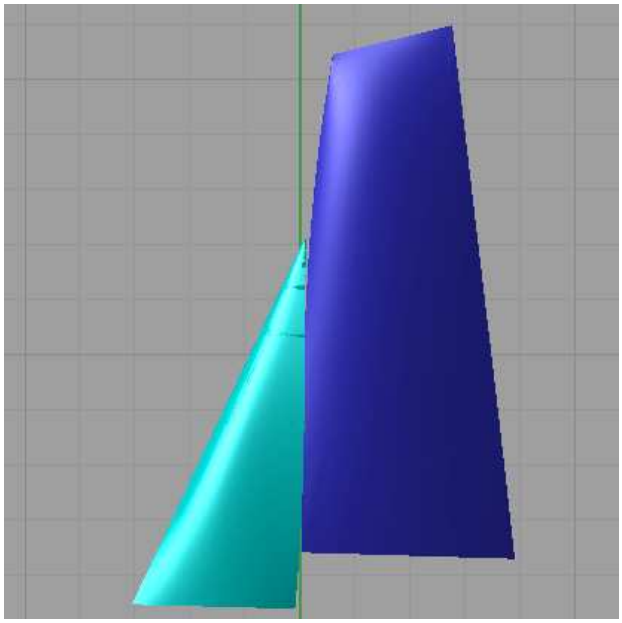

Figure 16: 18 footer rig

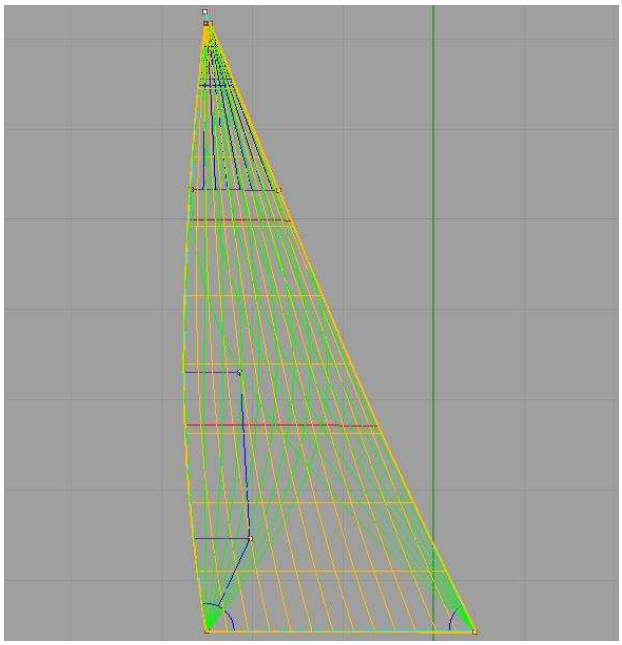

Figure 17: genoa design with all its geometric characteristics.

On this example, after only three iterations of the FSI loop between the structural and the aerodynamic codes (OpenFOAM used here) the convergence is good with less than a centimetre of difference between the two last sail shapes and less than 1% on driving and heeling forces between the two last iterations (see following table).

Aerodynamic loads convergence with FSI iterations:

	It.	Fr	Fh	Fr/Fh
Design shape	0	316	952	0.33
Flying shape	1	313	1077	0.29
“	2	305	1051	0.29
“	3	302	1045	0.29

The first difference between the design shape and the flying shape concerns the fullness of the sail: the sail moves downwind, the stay bend, the leech opens and the twist changes (figure 18).

Considering what happens at 20%, 40%, 60% and 80% high of the sail, we can see on figure 19 that the flying shape is less twisted than the design shape, with fewer camber. The camber moves forward.

Quantifications of these differences on sail shape are resumed in the following table:

	20%	40%	60%	80%
δ	11° - 14°	19° - 14°	24° - 16°	30° - 18°
f/c	8 – 7	13 – 10	17 – 13	20 – 15
x_f/c	39 – 38	33 – 28	35 – 26	40 – 27
α_i	44° - 46°	68° - 63°	79° - 70°	86° - 71°

The difference between global aerodynamic loads on the design and flying shapes is about 5% for the driving force and 10% for the heeling force. In this case, sail deformation decreases sail performances.

Another interesting point is that our flying shape is not totally smooth near the head (figure 20). So we have yet some work with the structural conception and the design of the sail to improve its performances and make the flying shape more efficient.

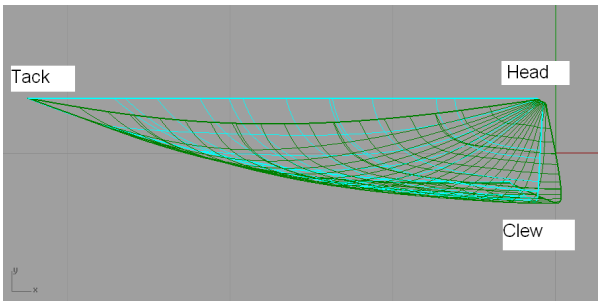

Figure 18: design shape (cyan) and flying shape (green)

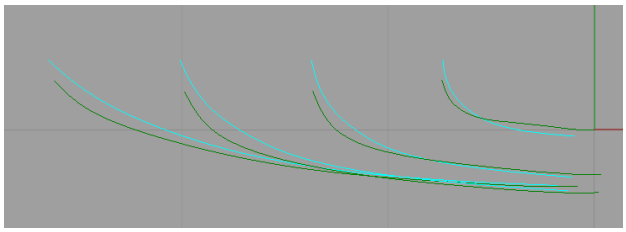

Figure 19: four sail cuts of the design and flying shapes

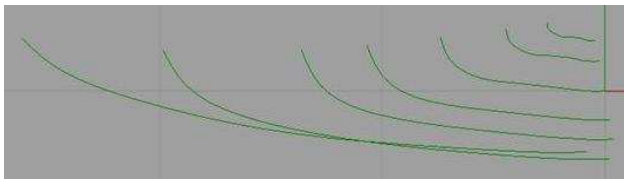

Figure 19: the sail has a weird shape near the head

8. CONCLUSIONS

ADONF, the computational framework developed for the three-dimensional simulation and optimization of flows around bodies through viscous RANS modelling is extended to fluid structure coupling in collaboration with Peter Heppel Associates. First results obtained in FSI mode have been presented to illustrate the ability to do multi-disciplinary analysis and optimization of sail flows through the coupling of viscous CFD and nonlinear structural modelling.

Main results are the followings:

- A user-friendly environment in development to run a large number of RANS simulations and to resolve multidisciplinary optimization problems about sails.
- An expertise in viscous flow modelling through numerical simulations and validations by comparisons with wind-tunnel results.

- A validated high-fidelity RANS solver with hybrid meshes to capture main flow features like separated flows on mast and mainsail configurations [13].
- A derivative free optimization algorithm based on evolutionary strategy implemented in ADONF for the search of optimal rigs for complex multi-modal rig configurations.
- A loose coupling FSI loop between an aerodynamic solver and RELAX a non linear structural solver.

This is the beginning of ADONF as a multidisciplinary computational framework. This opens new possibilities for flow analysis and optimization. In the future, more detailed and accurate validations through wind-tunnel tests comparisons on three dimensional sails or rigs will be needed.

9. REFERENCES

1. Gentry Arvel, "The Aerodynamics of Sail Interaction", *3th AIAA Symposium on the Aero/Hydronautics of Sailing*, November 1971.
2. Gentry Arvel, "A Review of Modern Sail Theory", *11th AIAA Symposium on the Aero/Hydronautics of Sailing*, September 1981.
3. Gentry Arvel, "The Application of Computational Fluid Dynamics to Sails", *Symposium on the Hydrodynamic Performances Enhancement for Marine Applications*, November 1988.
4. Marchaj C. A., *Sail Performance*, McGraw Hill, Great Britain, 1996.
5. Milgram J.H., "Sail Force Coefficients for Systematic Rig Variations", September 1971.
6. Milgram J.H., "Effects of Masts on the Aerodynamics of Sail Sections", Marine Technology, vol. 15(1), 35-42, 1978.
7. Jones P., & Korpus R., "International America's Cup class yacht design using viscous flow CFD", *SNAME 15th Chesapeake Sailing Yacht Symposium*, Annapolis, Maryland, USA, January 2001.
8. Korpus R., "Reynolds Averaged Navier-Stokes in an Integrated Design Environment", *MDY04 International Symposium on Yacht Design and Production*, Madrid, Spain, 2004.
9. Korpus R., "Performance Prediction without Empiricism: A RANS-Based VPP and Design Optimization Capability", *SNAME 18th Chesapeake Sailing Yacht Symposium*, Annapolis, Maryland, USA, March 2007.
10. Heppel P., "Accuracy in Sail Simulation: Wrinkling and Growing Fast Sails", *Proceeding of the 2nd High Performance Yacht Design Conference*, Auckland, New-Zeeland, December 2002.
11. Chapin V.G., "Gréement de l'Hydraplaneur - Gerris", Contract report n°2002-2, 2002.
12. Chapin V.G., Neyhousser R., Jamme S., "Aérodynamique grand voile - mât", *2nd Workshop Science & Voile*, Ecole Navale, Lanvéoc-Poulmic, May 2004.
13. Chapin V. G., Jamme S. and Chassaing P., "Viscous CFD as a relevant decision-making tool for mast-sail aerodynamics", *Marine Technology*, **42**(1), p1-10, 2005.
14. Chapin V. G., Neyhousser R., Jamme S. Dulliand G., Chassaing P., "Sailing Yacht Rig Improvements through Viscous CFD", *SNAME 17th Chesapeake Sailing Yacht Symposium*, Annapolis, Maryland, USA, March 2005.
15. Chapin V. G., Neyhousser R., Dulliand G., Chassaing P., "Analysis, Design and Optimization of Navier-Stokes Flows around Interacting Sails", *MDY06 International Symposium on Yacht Design and Production*, Madrid, Spain, March 2006.
16. Chapin V. G., Neyhousser R., Dulliand G., Chassaing P., "Design Optimization of Interacting Sails through Viscous CFD", *INNOVSail2008, Innovation in high performance sailing Yacht*, Lorient, France, May 2008.
17. Querard, A.B.G. and Wilson, P.A., "Aerodynamic of Modern Square Head Sails: A Comparative Study Between Wind-Tunnel Experiments and RANS Simulations", *The Modern Yacht, 2007*, 107-114.
18. Renzsch H., Graf K., "FlexSail – A Fluid Structure-Interaction Program for the Investigation of Spinnakers", *INNOVSail2008, Innovation in high performance sailing Yacht*, Lorient, France, May 2008.
19. Fossati F. & al., "Wind Tunnel Techniques for Investigation and Optimization of Sailing Yachts Aerodynamics", *Proceeding of the 2nd High Performance Yacht Design Conference*, Auckland, February 2006.
20. Fossati F., Muggiasca S., Martina F., "Experimental Database of Sails Performances and Flying Shapes in Upwind Conditions", *INNOVSail2008, Innovation in high performance sailing Yacht*, Lorient, France, May 2008.
21. Fossati F., Viola I.M., "Downwind Sails Aerodynamic Analysis", *In the proceedings of the 6th International Colloquium on Bluff Bodies Aerodynamics and Applications*, July 2008, Milan, Italy.

22. Graves W., Barbera T., Braun J.B., Imas L., "Measurements and Simulations of Pressure Distribution on Full Size Sails", *Proceeding of the 3rd High Performance Yacht Design Conference*, Auckland, New-Zeeland, December 2008.

23. Claughton A., "Development in the IMS VPP Formulations", *SNAME 14th Chesapeake Sailing Yacht Symposium*, Annapolis, USA, 1999.

24. Jackson P.S., "An improved upwind sail model for VPPs", SNAME 15th *Chesapeake Sailing Yacht Symposium*, Annapolis, USA, 2001.

25. Oossanen P. van, "Predicting the Speed of Sailing Yachts", SNAME Transactions, Vol 101, 337-397, 1993.

26. Teeters J. & al., "Changes to Sail Aerodynamics in the IMS Rule", *SNAME 16th Chesapeake Sailing Yacht Symposium*, Annapolis, Maryland, USA, March 2003.

27. Spalart, P.R., Allmaras, S.R., "A one-equation turbulence model for aerodynamic flows", AIAA paper 92-0439, 1992.

28. Gambit 2.3 & Fluent 6.2 users guide and tutorials, http://www.fluent.fr/

29. Wilkinson, S., "Partially Separated Flows around 2D Masts and Sails", PhD Thesis, University of Southampton, UK, 1984.

30. Wilkinson, S., "Static Pressure Distributions over 2D mast/sail geometries", Marine Technology 26, 4, 333-337, 1989.

31. Wilkinson, S., "Boundary Layer Explorations over a 2D mast/sail geometry", Marine Technology 27, 4, 250-256, 1990.

32. Barnes, M., "Form and stress engineering of tension structures". Structural Engineering Review Vol 6 No 3-4 175-202, 1994.

33. Desbrun, M., Meyer, M., Alliez, P., "Intrinsic Parameterizations of Surface Meshes", Vol 21, N°2, Eurographics 2002.

34. Rechenberg, I., Evolutionstrategie – Optimierung technischer Systeme nach Prinzipien der Biologischen Evolution, PhD thesis, 1971, reprinted by Fromman-Holzboog in 1973.

35. Pulliam T.H., Nemec M., Holst T., Zingg D.W., "Comparison of Evolutionary (Genetic) Algorithm and Adjoint Methods for Multi-Objective Viscous Airfoil Optimizations, AIAA paper 2003-0298, Reno, USA, 2003.

36. Hansen, N. and A. Ostermeier (2001). Completely Derandomized Self-Adaptation in Evolution Strategies. *Evolutionary Computation*, 9(2), 2001.

37. Hansen, N. and S. Kern (2004). Evaluating the CMA Evolution Strategy on Multimodal Test Functions. In *Eighth International Conference on Parallel Problem Solving from Nature PPSN VIII, Proceedings*, pp. 282-291, Berlin: Springer, 2004.

38. Müller S.D., "Bio-Inspired Optimization Algorithms for Engineering Applications", PhD Thesis, 2002.

39. Deb, K., "An efficient constraint handling method for genetic algorithms", *Computer Methods in Applied Mechanics and Engineering, 186*, 311-338, 2000.

40. Bethwaite F., "High performance sailing", Waterline Books, p209, 1996.

41. Kamakoti, R. and Shyy, W., "Fluid-Structure Interaction for Aeroelastic Applications", *Progress in Aerospace Sciences, 40*, 535-558, 2004.

10. AUTHORS' BIOGRAPHIES

Vincent G. Chapin, Associate Professor ISAE. Member of the "Advanced Aerodynamic & Control" team of the Aerodynamic Energetic and Propulsion Department of ISAE. His research is devoted to unsteady flows, innovating aerodynamic and flow control.

Nolwenn de Carlan, ENSICA student.

Peter Heppel, Engineer.